LU TP 10-18
June 2010

Tracer Particle Dynamics in Heterogeneous Many-body Systems

Master of Science Thesis by Karl Fogelmark
Thesis Advisor: Tobias Ambjörnsson

Abstract

By use of a lattice random walk algorithm we model diffusion in a many-body system and study the mean square displacement (MSD) for a tagged particle for different distributions of crowding particles, with particular emphasis on obtaining the correlation factor which contains the corrections to the mean-field result in such a system. The MSD in such a crowded environment is investigated and we find that the analytical correlation factor developed by Nakazato et al.[1] is not accurate for a tracer particle that is faster than the surrounding homogeneous crowding particles. Simulation results for the correlation factor is found for diffusion in a heterogeneous environment, where the friction coefficients of the crowding particles were drawn from a uniform distribution, and a power-law distribution. The simulation results can not be fitted to Nakazato's analytical form for the correlation factor. The MSD of a particle with the same diffusion constant as the crowding particles is investigated for a system where the particles have a probability, proportional to the corresponding Boltzmann factor, to form bonds to their nearest-neighbors. The MSD is found to be subdiffusive, (MSD$\propto t^{\delta}$, $\delta < 1$) and the exponent δ decreases almost linearly with increasing interaction strength and is roughly independent on the concentration of crowding particles.

LUND
UNIVERSITY

Department of Astronomy and Theoretical Physics
Lund University

1 Introduction

The cytoplasm of living cells is crowded by a large variety of different macromolecular species. This has a strong influence on the dynamics and equilibrium properties of the intracellular environment and changes chemical reaction rates, compared to what is measured during dilute *in vitro* experiments (experiments performed outside the cell). The typical concentration of crowding agents, such as proteins and nucleic acids, during in vitro experiments is less than 1 mg/ml. This is substantially lower than what can be found during *in vivo* experiments in living cells, where the concentration is in the range 50-400 mg/ml [2]. Although the concentration of each separate species is low, the combined volume occupied by these crowding macromolecules can be up to 40 % [3], distributed over a wide range of different sizes [4].

The reduction of available volume leads to altered reaction rates and equilibrium conditions for many different macromolecules. Understanding these crowded environments is important, since it is under these conditions all reactions within the cells take place. The reaction rate might initially increase due to the longer time the enzymes stay in close proximity to each other and increase the thermodynamic activity, but eventually the reaction rate is bound to be slowed by the subdiffusive kinematics of the system. The largest shifts in equilibrium constants can be seen for association of macromolecules where the equilibrium constants can increase several orders of magnitude compared to uncrowded situations [2, 5].

The recent progress in experimental techniques has increased the resolution of measurements down to the nanometer scale, and allows for tracking of single macromolecules. By the use of super-resolution fluorescence microscopy, single proteins inside living cells can be tracked at a resolution that far exceeds the normal diffraction limited microscopes ($\sim \mu m$). By tagging the object of study with a fluorescent molecule, and allowing only a few of the tagged particles to fluoresce at any given time, the electromagnetic interference between the tagged molecules is reduced. Although the technique has a few shortcomings, such as the photoactivation of the tagged molecule damaging the living cell, these can be considered as minor, as long as they are kept in mind when taking the measurements. The super-resolution technique is ideal for the study of the molecular heterogeneity in cells [6].

There are many experimental measurements of the mean square displacement (MSD) of a tracer particle in crowded environments showing a MSD of $\left\langle \delta r^2 \right\rangle = \Gamma t^\alpha$, with anomalous subdiffusive characteristics, i.e. $\alpha < 1$ [7]. During measurements carried out in E. coli. bacteria, the proportionality constant (Γ) was found to vary considerably for different cells and experimental conditions, but the exponent α was independent of particle size and background conditions [8].

For a review of crowding, there are numerous articles available. Fulton [9] gives an overview of the different indications of crowding, and Dix [4] has focused on the diffusion in crowded environments. Minton [2] and Ellis [5] discuss excluded volume, and the altered reaction rates, and Schnell et al. [3] gives a review of in vivo versus in vitro experiments, complemented with a simulation.

There are many in-depth articles on the various aspects of crowding. For experimental results on subdiffusion in cells, see ref. [8, 7, 10]. The Nakazato

and Kitahara paper from 1980 [1], on diffusion in two-species environments, is an undiscovered gem within the theoretical field, where they find an analytical expression for the diffusion constant. Their expression was later extended in ref. [11], and yet again in 2002 by Kitahara et al. to include diamond and honeycomb-lattices [12], and most recently by Kazuhiko [13] who included site blocking effects and the difference in concentration around each particle, where he also allowed for reactions between them. The MSD in a single file system (one dimensional) where the diffusing hard-core particles have different diffusion constants was investigated by Ambjörnsson et al. [14] and an analytical expression for the MSD was found, showing subdiffusion. In the early 80's Kutner et al. investigated diffusion and time correlation between consecutive jumps on a 3D fcc Bravais lattice, both with [15], and without [16] interaction. Later Kutner and Kehr [17] investigated the tracer diffusion coefficient on an fcc lattice, where the tracer particle had a different jump ratio relative the crowding particles. Jönsson [18] worked out an analytical expression for self-diffusion in colloidal systems with a varying concentration. Berry [19] performed a Monte Carlo simulation in order to investigate diffusion-limited enzyme reactions with varying obstacle concentrations.

However, the number of studies on heterogeneous environments, in higher dimensions ($d > 1$), is scarce. Most research in the field focuses on simplified models, where a number of parameters have been stripped down, such as dimensionality and/or homogeneity of the obstructing particles. We propose to change this, since living cells are crowded with a large variety of different macromolecules, and the diffusion in the cytoplasm transpires in several dimensions. We investigate these systems by constructing a stochastic algorithm, where many different hard-core interacting particles perform random walks on a d-dimensional lattice, where $d = 1, 2, 3$.

In section 2 we give a short introduction of the physics behind crowding, and section 3 details the simple dynamics of single particle systems, with a discussion on ergodicity. In section 4 we investigate a one dimensional system, with many particles, and in 5 we peruse the dynamics of hard-core interacting particles in two and three dimensions. The main contribution to the new frontiers of science is outlined in section 6, where we perform simulations of heterogeneous environments, and investigate the correlation factor for the MSD in such systems. Finally, section 7 is devoted to diffusion where the particles can interact. Details of the algorithm used and additional figures can be found in the appendix.

2 Excluded Volume

In order to gain a better understanding of how crowding changes the environment in biological cells, we need to understand the physics behind it. The crowding particles exclude a volume that is effectively larger than their own physical size, determined by their radius. The volume available to a particle can be defined as the fraction of space available to its center of mass. A small hard-core particle with radius r cannot be closer to a larger crowding particle (with radius R) than $R + r$, as can be seen in fig. 1.

When the distance between two large particles become comparable to the radii of the smaller particles, a short range attractive entropic force between

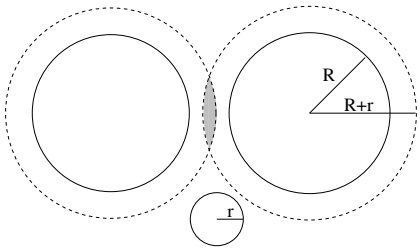

Figure 1: The center of the smaller particle is excluded from a distance $R + r$ from the center of the larger particles. When two areas of exclusion overlap (shaded area), the smaller particle will have a larger volume to move in. This causes an increase in entropy (more available states) and therefore a decrease in total free energy.

the large particles will result. As the region of excluded volume between two crowding particles overlap, the volume available to the smaller particle increases, causing an increase in the number of available configurations. This leads to a higher entropy, and consequently, a decrease in total free energy. Hence, binding events between particles are privileged, since these will lead to the maximal reduction of excluded volume [5, 20].

The exclusion of volume, due to crowding and its concomitant effects, causes significant changes in the intracellular environment. Not only will there be an attractive entropic force, but the chemical potential of the solute will also increase [4].

By discretizing space and time we get a lattice model that will retain the same long-time equilibrium conditions as the continuous system; however, we will not get any entropic force of the type above between the particles without explicitly adding interaction, since all particles take up the same amount of space. Since we wish to model a continuous infinite system we need to take many steps in time; at the same time we do not want the diffusion particle to "feel" the finiteness of the lattice. These are all concerns to which we must abide.

3 Single Particle Systems

We have simulated a one-particle system by performing a random walk, with constant jump length, on a cubic lattice with fixed boundary conditions, in one, two and three dimensions. For each ensemble the particle starts from the center of the lattice, and makes a jump each time unit, in a random direction (each dimension has two possible directions).

3.1 Ergodicity

Since time in our model is discretized, it is important to keep in mind for which timescales the finite lattice and discretized time effect our model not to correspond to an infinite continuous system. For times t in the interval $t_{\min} \ll t \ll t_{\text{eq}}$, where $t_{\min}$ is the time between each jump, the MSD is given by

the usual diffusion law for Brownian motion:

$$\left\langle \delta r^2 \right\rangle = 2dDt, \tag{1}$$

where the displacement from the starting coordinate (r_0) is defined as $\delta r = r_0 - r$, d is the dimensionality, and D is the diffusion constant. For short times ($t_{\min}$) the system has not had time to relax (insufficient amounts of steps). Conversely, the upper bound for t is the equilibrium time t_{eq}, characterized by the time it takes for the system to become ergodic, which is $t_{\text{eq}} = \frac{(L/2)^2}{2D}$, since the particle is placed at the center of the lattice, a distance $L/2$ from the box boundary, where L is the side length of the lattice.

The mean square displacement for the system at times $t \gg t_{\text{eq}}$ will only depend on the lattice size. When the system becomes ergodic each site will be accessible to each particle (if more than one), with identical probability, P_ν, for each state (i.e. site) ν. The mean square displacement, $\left\langle \delta r^2 \right\rangle$ for a particle diffusing over a discrete lattice of $L_x \times L_y \times L_z$ sites, can thus be written as:

$$\left\langle \delta r^2 \right\rangle = \sum_\nu P_\nu \delta r^2 = \frac{1}{L_x L_y L_z} \sum_{i=1}^{L_x} \sum_{j=1}^{L_y} \sum_{k=1}^{L_z} (x_i - x_0)^2 + (y_j - y_0)^2 + (z_k - z_0)^2 \tag{2}$$

where x_0, y_0, z_0 are the starting coordinates. Each sum (dimension) will give a contribution to the final MSD of[1]

$$\left\langle \delta x^2 \right\rangle = \frac{1}{6}(L_x + 1)(2L_x + 1) + x_0^2 - x_0(L_x + 1). \tag{3}$$

From figure 2 we can see that our simulations are in good agreement with this result. For short times, ($t \ll t_{\text{eq}}$), the particle undergoes diffusion, in agreement with (1).

4 Many Particles in One Dimension

The dynamics of a one dimensional crowded system has many interesting aspects. The diffusion of proteins along a DNA chain can be seen as a one dimensional system, and since the hard-core particles cannot pass each other, their order is always preserved.

In order to simulate crowding on a lattice we model a stochastic system (as in section 3), with a number of additions to allow crowding. For each ensemble, the tagged tracer particle is placed at the center of the lattice, and the remaining $N - 1$ crowding particles are randomly distributed over the vacant sites, under the constraint that the lattice only allows for single occupancy of each site. Each particle is assigned an isotropic jump rate k_i, drawn from a predetermined probability distribution $\varrho(k_i)$, by using the *trail-and-error* procedure outlined in ref. [14], which draws particles proportional to their hop rate k_i ($i = 1, \ldots, N$). The system is quenched, meaning that the jump rates are the same for all ensembles. For each moved particle, or attempted move, the time is updated by $t = t + \frac{1}{P_{2dN}}$, where P_{2dN} is the sum of all jump rates. The vacant sites represent the solvent, and for each particle collision the moving particle is moved back to

[1] See appendix A for further details, p. 21.

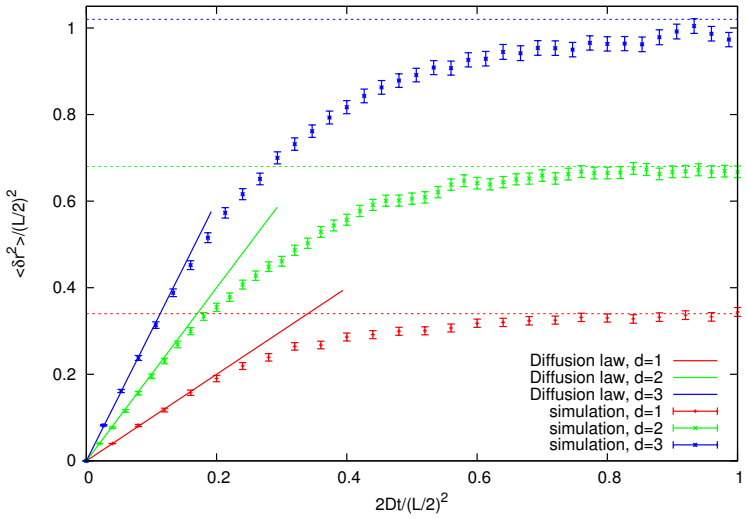

Figure 2: Self diffusion for a single-particle in a box with side length $L = 10$, consisting of L^d lattice points, where d is the spatial dimension of the system. The system shows normal diffusive behavior (see eq. (1)) until it approaches the limit of ergodicity. The horizontal lines corresponds to eq. (2) & (3) for the parameters used in our simulations. The MSD was averaged over 1000 ensembles, and the starting coordinates for the particle was taken as $L/2$. The error-bars are the standard error.

its previous position, thereby earning the name "trial-and-error", and the next particle to be moved is chosen, in accordance with the jump rate distribution.[2]

Due to the crowding particles, the shortest characteristic time is now modified, compared to the one particle system, to be the average time between particle collisions τ_{coll}. A fast particle (large jump rate k_i) will collide more frequently, likewise, a system with higher concentration (N/L) will also shorten τ_{coll}. With a lattice constant $a = 1$, and the relation between jump rate and diffusion constant of particle i as $k_i = D_i/a^2$, we can write the typical collision time as $\tau_{\text{coll}} = \frac{L^2}{2N^2 D_{\text{eff}}}$, where D_{eff} is the effective diffusion constant, given by $D_{\text{eff}}^{-1} = N^{-1} \sum_{i=1}^{N} D_i^{-1}$.

4.1 MSD in a Crowded One-dimensional System

The effective diffusion constant (D_{eff}) introduced above, is equivalent to the inverse average friction constant, which determines the long-time ($t \gg \tau_{\text{coll}}$) behavior of the MSD. The friction coefficient is related to the (free particle) diffusion constant according to the Einstein relation as $\zeta = k_B T/D$, where we take $k_B T = 1$, for convenience. The MSD dependence on D_{eff} was found in ref. [14], where the MSD was given by:

$$\langle \delta x^2 \rangle = \frac{1-c}{c} \sqrt{\frac{4 D_{\text{eff}} t}{\pi}}, \tag{4}$$

[2]See appendix B.1 for further details on the algorithm used, including the trial-and-error method.

where we define the concentration c as particles per total number of lattice sites $c = N/M$. The system shows (non-linear) subdiffusive characteristics; where the MSD is proportional $\sqrt{t}$. From figure 3 we see good agreement with our simulations, where we have simulated a system with identical jump rates (homogeneous), and two heterogeneous ones, where the friction coefficients were drawn from a power-law distribution, with a finite first moment, and an exponential distribution.

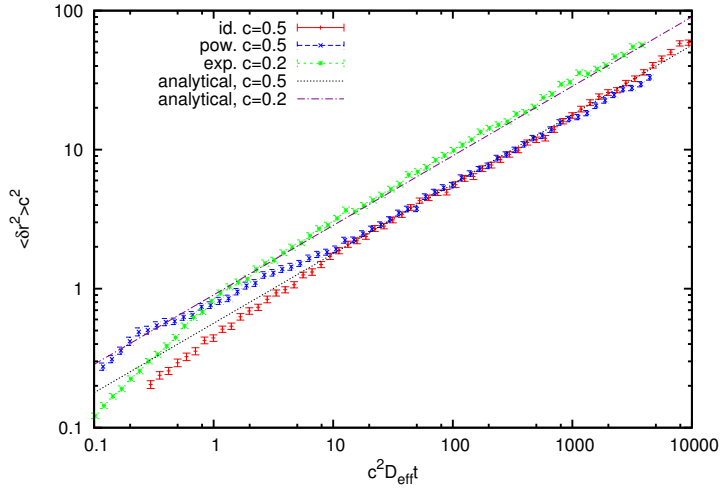

Figure 3: MSD (on a log-log-scale) as a function of time, in a one dimensional system consisting of 100 lattice sites. The agreement between the simulation and the analytical expression (eq. (4)) is good for times $t \gg \tau_{\text{coll}}$. Two simulations were made with concentration $c = 0.5$, one with identical particles $k_i = 1 \; \forall \, i$, and one with a power-law distributed friction coefficient (with finite first moment, $\alpha = 1$). A third simulation was made with friction coefficients drawn from an exponential distribution, with $c = 0.2$. All simulations were averaged over 1000 ensembles, and the jump rate of the tracer particle was $k_t = 0.01$.

4.2 Power-Law Distributions

The diffusion equation relies on the central limit theorem, which states that the distribution of the displacement of the particles is Gaussian, as long as the second and first moment of the displacement is finite, and Markovian, i.e. each move is independent of the previous one. Since we are interested in anomalous (sub) diffusion, MSD $\propto t^{\delta}$, ($\delta < 1$), we stand to gain by choosing our friction coefficients ζ_i (inverse jump rates $k_i = \zeta_i^{-1}$) from a power-law distribution, $\varrho(\zeta) \propto \zeta^{-1-\alpha}$, where the second moment is infinite for $0 < \alpha < 2$. For $0 < \alpha < 1$ the first moment will also tend towards infinity, giving rise to a long "heavy tailed" distribution.

We generate the power-law distribution by using the continuous transformation method where the cumulative distribution is given by $C(\zeta_i) = \int_0^{\zeta_i} \varrho(\zeta')d\zeta'$. This allows us to generate friction coefficients with a power-law distribution from a uniformly distributed random number, $0 < R < 1$, by $\zeta_i = R^{-1/\alpha}$.

5 Many-Particles in Higher Dimensions

The dynamics of a crowded system in two and three dimensions, where the crowding agents all have the same jump rate k_c, and the tagged particle has another jump rate k_t, is well understood, and the analytic expression for the diffusion constant was outlined in ref. [1] by Nakazato and Kitahara. Since the probability for a site to be occupied is equal to the concentration c, crowding will, to a first (mean field) approximation, reduce the self-diffusion constant by an amount proportional to the fraction of volume occupied by the particles, $D = D_0(1-c)$, where $(1-c)$ is the probability of the target site being vacant, and D_0 is the diffusion constant in the limit $c \to 0$. In the mean field approximation the tracer particle is considered to move in an average background of identical particles, with a jump rate $(1-c)k_t$, where k_t is the original jump rate of the tracer particle in a one-particle system. For a two species system we get linear diffusion, but the diffusion constant in eq. (1) for the tracer particle is modified as:

$$D = k_t a^2 (1-c) f(c,k), \tag{5a}$$

where a is the lattice constant, and $f(c,k)$ is the correlation factor (with $k \equiv k_t/k_c$), that relates the correlation between consecutive jumps, and is given by

$$f(c,k) = \frac{[k(1-c)+1][1-\alpha]}{k(1-c)+1-\alpha(1+k(1-3c))} \tag{5b}$$

which was the main result in Nakazato's article, a result they got by applying a saddle point approximation to the solution of the many-particle master equation. Here, $\alpha = 1$ for one dimension and $\alpha = 0.363$, $\alpha = 0.209$ for two, and three dimensions, respectively. For $c \to 0$, $f \to 1$ and we get the normal diffusion law: When the tagged particle is much slower than the crowding particles, $(k \to 0)$ the correlation factor becomes unity, since the rapidly fluctuating background removes any correlation. Conversely, when the tracer particle is much faster than the crowding agents, $(k \to \infty)$ the correlation factor tends towards a finite value (< 1), since the tagged particle will be confined by the surrounding media that now constitute an immobile obstacle, thereby effectively trapping the tracer particle, that will have higher probability of jumping back to its previous position. More precise, for an environment with immobile particles $k_c = 0$, the correlation factor tends towards the finite value

$$\lim_{k\to\infty} f(c,k) = \frac{(1-c)(1-\alpha)}{(1-c)-\alpha(1-3c)}.$$

From equation (5b) we see that for one dimensional systems ($\alpha = 1$) the diffusion constant becomes zero, i.e. the linear term disappears and we get subdiffusion, as was shown in eq. (4). In figure 4 we see good agreement with our simulations, performed in two and three dimensions, for $k < 1$.

However, the Nakazato expression (5) is based on a statistical averaging procedure, and is not correct for all jump ratios. When the tagged particle is faster than the surrounding media, $(k > 1)$ the actual correlation factor deviates from eq. (5). In figure 5 we notice a deviation between the analytically predicted MSD compared to what was obtained from simulations. From these results we are led to investigate this discrepancy further, by running simulations with jump ratio $0.5 \leq k \leq 6$. The result can be seen in fig. 6, which shows that eq. (5b)

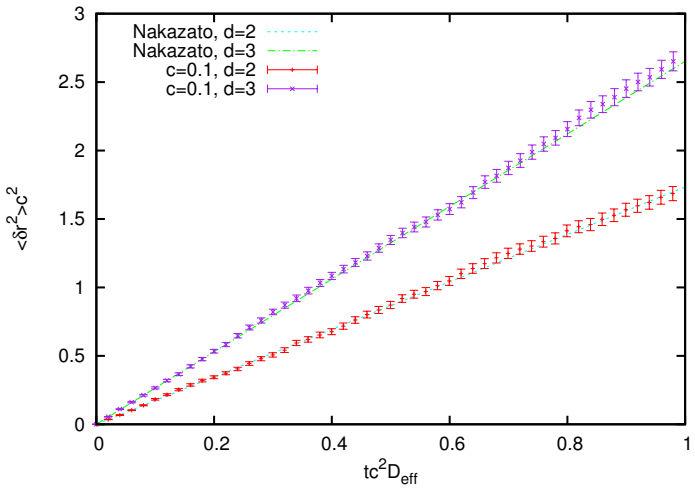

Figure 4: Diffusion in a two species environment, with MSD plotted against time. Both simulations were performed on a d-dimensional lattice with 100^d sites. We see a good agreement with the Nakazato-equation (5), represented by the dashed lines. The MSD was averaged over 1000 ensembles, with jump ratio $k = 0.5$, and concentration $c = 0.1$.

works well for $k < 2\ \forall c$, but once $k \geq 3$ and $c \geq 0.4$ the relative difference between the analytical solution and the simulation result exceeds 10 %, which indicates that Nakazato's expression needs to be modified in order to yield a result in accordance with our simulations in this interval.

5.1 Percolation

As the crowding species becomes immobile ($k \to \infty$), and the concentration increases, the system will eventually reach the percolation threshold, where a single continuous cluster of crowding particles will span the entire system. In the mathematical literature our algorithm is referred to as *a blind ant in the labyrinth*, since the ant (particle) does not know in advance whether the target site it is moving to is occupied or not. The percolation threshold can be seen as a second order phase transition, where the system makes a transition from a disconnected state, where no cluster is large enough to span all sides of the lattice, to a connected state. For an infinite two-dimensional square lattice this phase transition occurs at the critical concentration $c_p = 0.5927$, where c_p usually is defined as the occupational probability, resulting in a varying N for each ensemble in a simulation (grand canonical ensemble); note that in our simulations N is a fixed number (canonical ensemble) [21]. However, since the particle is diffusing over the vacant sites it is the percolation of vacancies, at particle concentration $\bar{c}_p = 1 - c_p$, that will set the limit for when the tracer particle will be confined [22].

For particle concentrations above $\bar{c}_p$ no vacancy cluster will be able to span all sides of the lattice, and the confining vacancy cluster will have a radius of the same order as the correlation length. Therefore the the tracer particle must

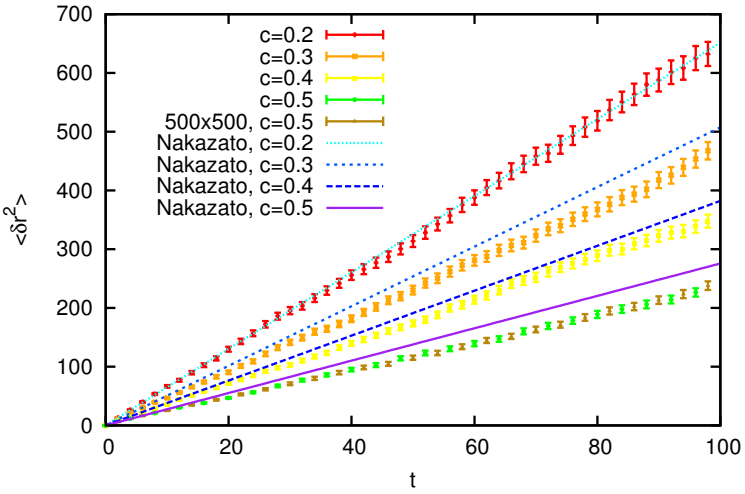

Figure 5: MSD of a tracer particle in a two-species environment, where the jump ratio is $k = 5$. A noticeable deviation between Nakazato's analytical correlation factor (5) (dashed lines) and the simulated result (marks with error-bars) is evident as the concentration increases. The simulations were performed on a 200×200 lattice, and for reference one simulation (with $c = 0.5$) was performed on a 500×500-lattice, to make sure $t \ll t_{\text{eq}}$. The marks with error-bars are the simulation results, where we averaged over 1000 ensembles.

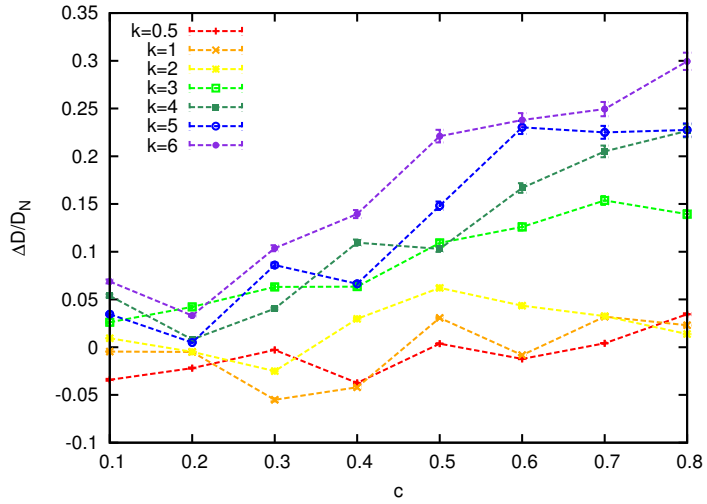

Figure 6: Relative difference of the simulated (D_{sim}) and the analytical (D_N) diffusion constant from eq. (5) for two-species crowding in two dimensions, for different concentrations ($\Delta D = D_N - D_{\text{sim}}$), and jump ratios $k = k_t/k_c$. The Nakazato expression is too moderate in its estimation, and the error increases with higher jump ratios and concentrations. The random walk was performed on a 200×200-lattice and the MSD was averaged over 1000 ensembles. The jump rate of the crowders was held constant, at $k_c = 0.5$.

asymptote to a constant value [23],

$$\left\langle \delta r_\infty^2 \right\rangle \approxeq |c - \bar{c}_p|^{-\kappa}, \tag{6}$$

where κ is a critical exponent. From figure 7 we see that $\left\langle \delta r_\infty^2 \right\rangle$ becomes larger the closer we get to $\bar{c}_p$, which is in agreement with (6). Furthermore, the functional form of the MSD will be [23]

$$\left\langle \delta r^2 \right\rangle \approx \left\langle \delta r_\infty^2 \right\rangle \left[1 - \exp\left(-bt^\beta\right)\right]. \tag{7}$$

Note that the apparent initial power-law behavior in figure 7 is due to the first order term in the Taylor expansion of eq. (7).

At the percolation threshold the motion is subdiffusive and the MSD will be proportional to t^δ, which seems to be in good agreement with our simulation results, with $\delta = 0.73$, in figure 7 [23].

For systems below the percolation threshold ($c < \bar{c}_p$) the tracer particle can still be confined to a smaller subsystem of unoccupied sites, which will initially cause a nonlinearity in the MSD that will persist the closer we get to the percolation threshold. For large times we get a linear MSD, even close to the percolation threshold, as can be seen in figure 7.

In order for the system to show percolative properties the crowding particles must be completely immobile. If $k < \infty$ the confining cluster will eventually reform, and in the process the tracer particle will escape. This gives rise to a monotonically increasing MSD, as can be seen in figure 8. The MSD is linear for times $t \gg 1/k_c$ [17].

6 Many-Particles: Beyond the Nakazato-Model

We have seen that the model presented by Nakazato and Kitahara in 1980 accurately describes the MSD of a two species system (for $k < 1$), in two and three dimensions, where the tracer particle is the sole constituent of one of the two species. We will now go one step further and investigate the behavior of the MSD for a system consisting of a tracer particle in a bath of different molecules. In order to investigate diffusion in these more heterogeneous distributions we make the initial hypothesis that the MSD will be of the same form as described by equation (5), but with a different correlation factor, which we wish to determine. As we shall see, this will not work.

The simulations were performed using the same algorithm as in section 4. Due to the now faster tracer particle (simulations were made up to $k_t \leq 6$), and the computationally heavy system, we take special care to stay below $t \ll t_{\text{eq}}$, which we ascertained by comparing simulations made on different lattice sizes, but with the same concentration (see appendix C for details, p. 24).

6.1 Uniformly Distributed Species

In our first simulation we draw the jump rates of the crowding agents from a uniform probability distribution such that $0 < k_c < 1$. This results in an averaged jump rate $\langle k_c \rangle = 0.5$, which we use to substitute k_c in eq. (5b). The behavior is diffusive (linear) for all tracer jump rates and crowding concentrations, as can be seen from fig. 9. Further investigation of the concentration dependence of

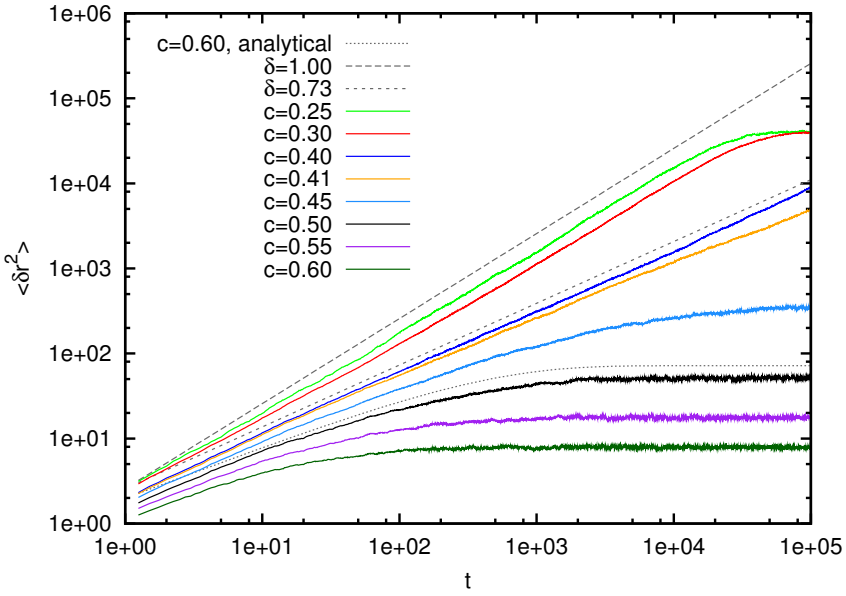

Figure 7: The MSD, on log-log scale, of a tracer particle in a 500×500-lattice system with immobile crowding particles ($k_c = 0$). The non-linear behavior is the effect of all tracer particles contributing to the MSD until they "feel" the finiteness of the confining vacancy cluster in which it diffuses. The unskilled scientist might mistake the non-linear onset above $\bar{c}_p$ as a true asymptotic power-law, however eq. (7) shows the true functional form (as a stretched exponential function). For clarity we include (7) (least-squares fitted, giving $\alpha = 0.61$) for $c = 0.60$, with a slight shift. For $c > \bar{c}_p$ the MSD asymptotes to eq. (6) and for $c = \bar{c}_p$ the MSD can be fitted to t^δ (doing so for this simulation yields $\delta = 0.73$, included in the figure with a slight shift). For $c \leq 0.30$ the tracer particle diffuses normally until it reaches equilibrium. The MSD was averaged over 1000 ensembles.

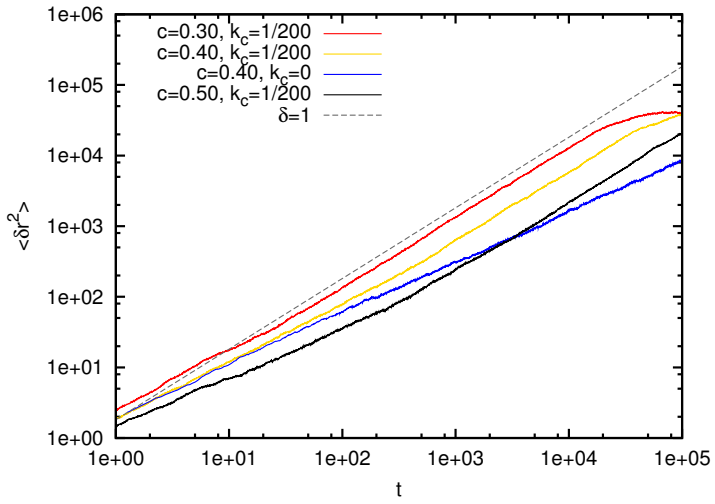

Figure 8: MSD of a tracer particle in a system with $k < \infty$, on log-log scale. The tagged particle will diffuse monotonically, even above the percolation threshold of the vacancies ($\bar{c}_p = 0.40$), since the now mobile, but slow, crowding species will cause the confining clusters to reform, which can be seen in the figure where we included $k_c = 0$, $c = 0.40$ (from fig. 7), for comparison; the MSDs will start to differ first after $t = 1/k_c$. The MSD was averaged over 1000 ensembles.

the diffusion constant shows that it is roughly linear, as can be seen in figure 16, in the appendix (p. 26).

As seen in fig. 10, the correlation factor from our simulations has a form similar to the Nakazato expression, but it cannot be fitted to it by changing the definition of the jump ratio k, which is the only parameter in eq. (5b) that we are free to change. Initially we chose $k = k_t / \langle k_c \rangle$, where $\langle k_c \rangle = 0.5$, to be the proposed form of the correlation factor, but it does not fit the simulated values, and changing k does not improve the overall fit, as can be seen from the figure.

From our results in figure 10 we can draw a number of conclusions. It appears as if the Nakazato expression, with the original jump ratio in eq. (5b) redefined as $k = k_t / \langle k_c \rangle$, is overestimating the values at high tracer particle jump rates. If we lower the value of k_c, thereby effectively increasing the k-parameter in (5b), we get a better fit in this region. We can interpret this as giving more statistical weight to the slower particles that will impede the path of our faster tracer particle. By a similar argument we can see that the opposite holds true; for a slow tracer particle the speed of the adjacent ones bears less weight. However, we should keep in mind that the Nakazato expression is not a good approximation for higher jump ratios (k), as was previously shown.

As a concluding remark, we note that the analytical correlation factor (5b) does not have the correct functional form for this system of non-homogeneous crowding particles. We need a new analytical expression for these more diverse systems, in order to increase our understanding of them.

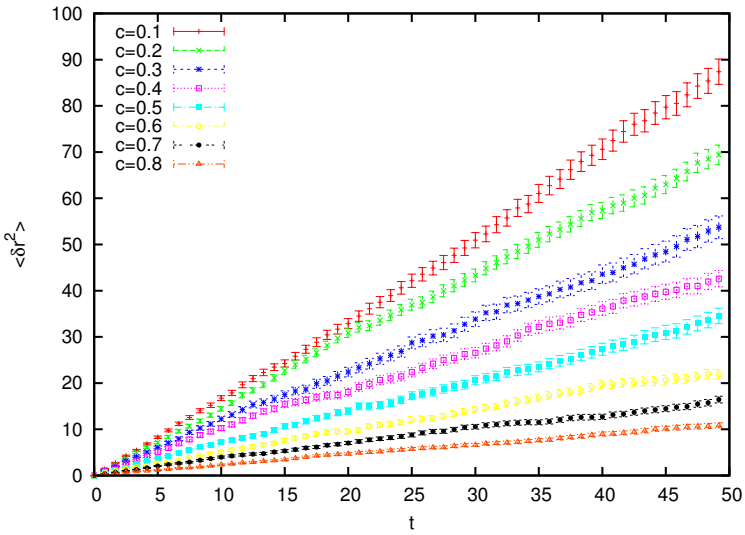

Figure 9: Mean square displacement on a two dimensional lattice, for a tracer particle with jump rate $k_t = 0.5$. The displacement is linear in time, and shows a substantial decrease for higher concentrations. All simulations were made on a 100×100-lattice, with a uniform distribution of k_c, $[0 < k_c < 1]$, and the MSD was averaged over 1000 ensembles. See appendix E.2 for more results.

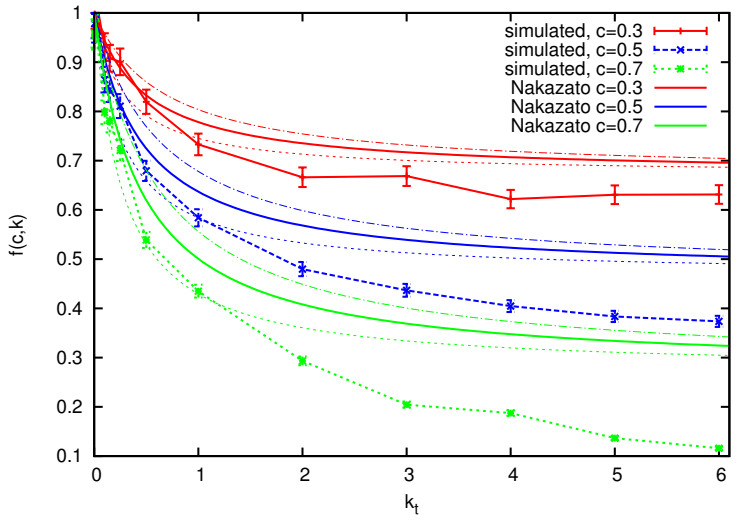

Figure 10: The correlation factor as a function of tracer jump rate, at concentrations $c = 0.3$ (red), $c = 0.5$ (blue), and $c = 0.7$ (green). The Nakazato correlation factor (eq. 5b) can not be fitted to our simulated values by simple manipulation of $k = k_t/k_c$ (dashed lines represent $k_c = 0.3$, dot-dashed $k_c = 0.7$, and the full lines $k_c = 0.5$). Our simulation outcome shows the same characteristics as the analytical correlation factor (5b), in the limit: $\lim_{k\to 0} f = 1$, as it should. The jump rates of the crowders were drawn from a uniform distribution, $[0 < k_c < 1]$, and the lattice comprised 100×100 sites.

6.2 Power-Law Distributed Species

Following the discussion in section 4.2, we do the same simulation as in the previous subsection, but with the inverse jump rates of the crowding species drawn from a power-law distribution rather than a uniform one. We choose $\alpha = 0.5$, meaning that neither the first nor the second moment will be finite, resulting in a power-law tail with slow jump rates. All simulations performed show a linear ensemble averaged MSD, as can be seen in appendix E.3.

The results for the correlation factor from our simulation can be seen in figure 11, where we notice that the behavior of the correlation factor resembles what could be seen in the uniform distribution (fig. 10). When comparing our result with an analytical expression, we used eq. (5b), where we interchanged the original k_c with the average jump rate of the crowding particles which was $k_c \approx 0.33$.

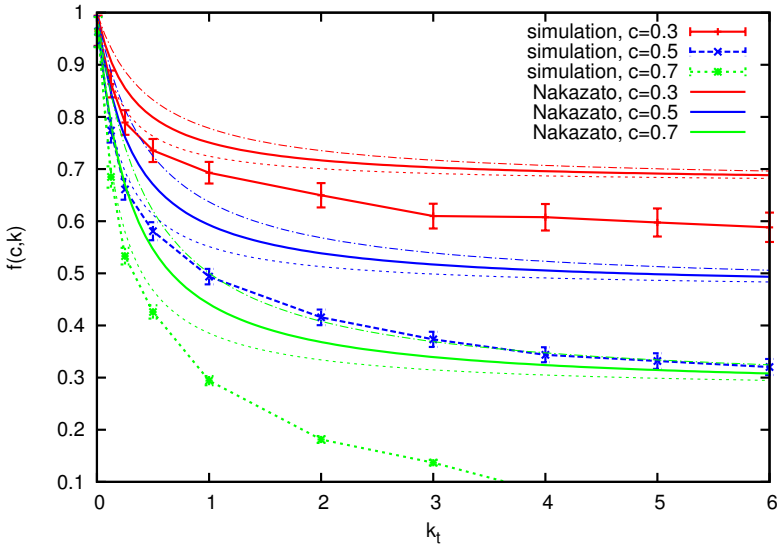

Figure 11: Correlation factor at concentration $c = 0.3$, $c = 0.5$ and $c = 0.7$, plotted against tracer the jump rate for diffusion in a system where the crowding agents have a friction coefficient with a power-law distribution (with $\alpha = 0.5$). As in the uniform case (fig. 10), the analytical correlation factor (5b) cannot be fitted to the simulation result. The dashed lines represent the analytical result with $k_c = 0.2$, the dot-dashed $k_c = 0.5$, and the full lines are the original fit with $k_c = 0.33$. All simulations were performed on a 100×100 lattice, and averaged over 1000 ensembles. For restrictions on the maximum number of time steps ($t \ll t_{\text{eq}}$), see appendix C.

The correlation factor decreases faster with increasing k_t for the power-law distributed system than for the uniform. This is not surprising since the crowding particles are slower for this simulation than the uniform one, and obstruct the tracer particle more. Notice that the correlation factor can be as small as ~ 0.1 (for the particles used in the simulation), which is far from the mean field result that would have $f(c, k) = 1$.

7 Interactions in a Homogeneous Crowded Two Dimensional System

As an extension of the previous simulations we add interactions between the particles, to model electrostatic and hydrophobic forces that can attract particles to form clusters. We allow the jumping particle to bond with its nearest-neighbors with a probability determined by the Boltzmann factor:

$$\exp(-n\beta\Delta\Phi)$$

where n is the number of nearest-neighbors ($n \leq 3$, when $d = 2$, or else there is no vacant site), and $\beta = (k_B T)^{-1}$ where k_B is Boltzmann's constant and T the temperature. The algorithm used follows the same structure as the previous code (see section 4), but with the additional extension that allows us to count the number of nearest-neighbors (n), for each move, and only accept the move if $R \leq \exp(-n\beta\Delta\Phi)$, where R is a uniformly distributed random number $0 < r < 1$. In order to reduce the intricacy of the problem, we give all particles a constant jump rate ($k_c = 1$).

The reduced dynamics of the system will no longer be of collision-type (steric obstruction) as was the case in the previous algorithm, but rather through the binding of particles in the vicinity of the moving particle to form clusters that reduce the overall speed. Unlike before (in the hard-core interacting case) the particles will not be at equilibrium at $t = 0$, due to their tendency to form clusters, which is not included when we randomly place the particles on the lattice. From figure 12 we see how the increase in interaction energy ($\beta\Delta\Phi = 6$) and concentration ($c = 0.8$) causes the particle to get stuck, and stay immobile for long periods of time. The MSD goes from linear ($\langle \delta r^2 \rangle \propto t^\delta$, $\delta = 1$) to subdiffusive ($\delta < 1$) as the interaction strength increases.[3] However, interestingly the exponent δ depends mainly on the dimensionless interaction strength $\beta\Delta\Phi$ and not significantly on the concentration c as can be seen from figure 13. The values in the figure were obtained by making a large number (10^4) of least-squares fittings ($\propto t^\delta$) to the MSD simulation values. For each fit the MSD values were modified by $\langle \delta r(t)^2 \rangle + R\sigma(t)$, where $\sigma(t)$ is the standard deviation of our simulated MSD at time t, and R is a normally distributed random number. For each of our MSD simulations we get 10^4 values for the exponent δ_i, which will have a Gaussian distribution, from which we get our plotted δ-value and its standard error.

8 Summary and Discussion

In this thesis we have simulated the random walk of a tracer particle in a crowded environment. In section 4 we found good agreement between our simulations and the analytical expression (4) for the long-time mean square displacement of a tracer particle in one dimension. It shows us that the algorithm used for the simulations is in agreement with the theoretical predictions. For higher dimensions we compared our simulation results with equation (5), which was derived for a two species system by Nakazato et al. and we found that we needed

[3] See appendix E.4 for more simulation results.

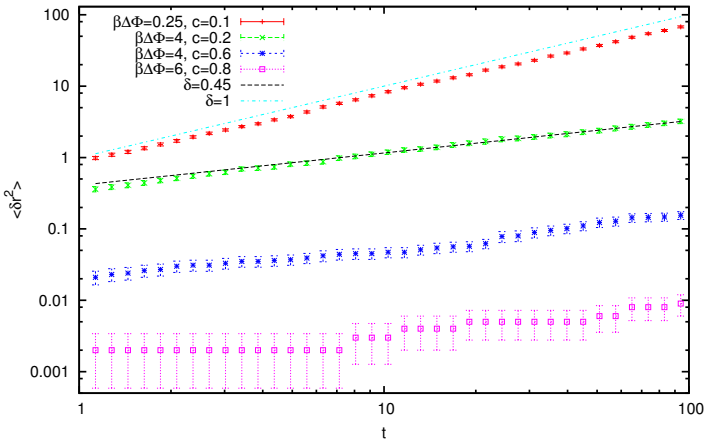

Figure 12: The MSD of a tagged particle with nearest-neighbor interactions on a log-log scale. For low densities and interaction strength the MSD is linear (see $\delta = 1$ line for comparison), but for higher strength ($\beta\Delta\Phi \approx 4$), we get subdiffusion. At high concentrations ($c \gtrsim 7$) the tagged particle will always have several neighbors, thereby increasing the probability of getting stuck. This is especially noticeable at $c = 0.8$ and $\beta\Delta\Phi = 6$. All simulations were performed on a 100×100-lattice, and the MSD was averaged over 1000 ensembles.

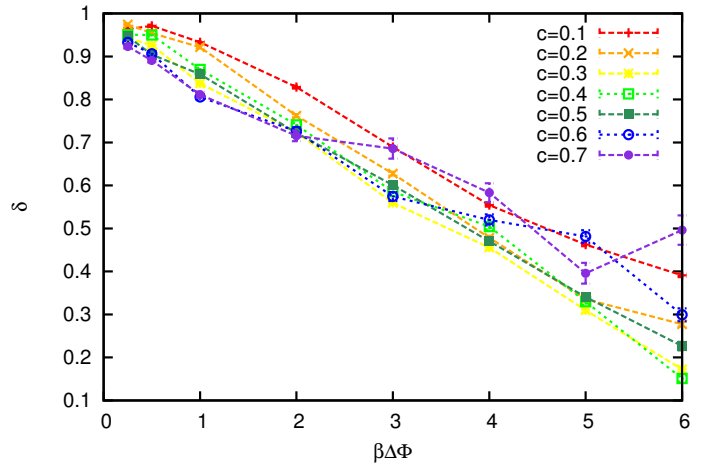

Figure 13: The exponent δ in the MSD $\propto t^{\delta}$ as a function of interaction potential. The exponent δ decreases almost linearly with $\beta\Delta\Phi$ and is roughly independent of concentration. All simulations were made on a 100×100-lattice, and the exponent δ was obtained by averaging many least-squares fittings, with Gaussian distribution, for each δ-value (see main text).

a better analytical correlation factor for when the tagged particle is faster than the surrounding homogeneous crowding particles.

The main purpose of this study was to investigate the correlation factor for the MSD of a tracer particle in a heterogeneous environment. We found that the correlation factor did not have the same functional form as the Nakazato equation (5b) when we drew the friction constants of the crowding particles from a uniform, or a power-law, distribution and it could not be fitted to the simulation results.

The algorithm we used was an attempt to capture the essential physics of a crowded system, and find out if we could model it in a way that would result in a subdiffusive MSD, not only for one dimension, but also for two and three. In order to do so we introduced a number of simplifications to increase computational speed. For instance, we only made jumps in directions along the coordinate axis, and always with constant jump length. Furthermore, we neglected long range potentials, and the effects of giving the different particles a volume that would be consistent with their radius, which could have been done by use of Stoke's law. However, our random walk has the desirable trait that it shares the same stochastic behavior as the Brownian motion of the individual particles, and our discrete lattice model has the same long-time characteristics as a continuous system.

As an expansion of our previous simulations we investigated the MSD of a homogeneous system where we included interactions between the particles. The nearest-neighbors of each moving particle had a probability proportional to the Boltzmann distribution of forming a bond to it, thereby slowing down the dynamics; we found that the tagged particle subdiffuses with an MSD exponent δ dependent of the interaction strength. This approach has a number of shortcomings. Firstly, the model is not physical when the interaction energy tends towards infinity since all particles will form a single immobile cluster, rather than a mobile one. Secondly, the clusters cannot break into more than one particle at a time, rather than breaking into two new clusters where each contains more than one particle. In appendix B.2 we propose an improved method for modeling interactions between particles, one that does not have these shortcomings. Computationally it is slightly heavier, but makes up for it by not sharing any of the undesirable traits of the code used in section 7.

We have pinpointed the need for further analytic work that can accurately describe the correlation factor for a heterogeneous system, as well as for a two species system with a jump ratio $k > 1$. There is still much to be done, and we hope to be able to continue our study, and put the proposed improved algorithm in appendix B.2 to work. Also, an analytic expression predicting how δ depends on the interaction strength for the case of interacting particles have yet to be derived.

Acknowledgments

I would like to thank my supervisor Tobias Ambjörnsson for invaluable guidance, advice, and for many rewarding discussions. I would also like to thank my former teachers, Hans-Uno Bengtsson (†), Bo Söderberg, and Stig Wramdemark for unveiling the mysterious nature of physics.

References

[1] K. Nakazato and K. Kitahara. Site blocking effect in tracer diffusion on a lattice. *Prog. Theor. Phys.*, 64(6):2261–2264, 1980.

[2] A.P. Minton. The influence of macromolecular crowding and macromolecular confinement on biochemical reactions in physiological media. *J. of Biolog. Chem.*, 276(14):10577–10580, 2001.

[3] S. Schnell and T.E. Turner. Reaction kinetics in intracellular environments with macromolecular crowding: simulations and rate laws. *Prog. Biophys. & Molecular Biology*, 85:235–260, 2004.

[4] J.A. Dix and A.S. Verkman. Crowding effects on diffusion in solutions and cells. *Annu. Rev. Biophys.*, 37:247–263, 2008.

[5] R.J. Ellis. Macromolecular crowding: obvious but underappreciated. *TRENDS in Biochemical Sciences*, 26(10):597–604, 2001.

[6] J. Lippincott-Schwartz and S. Manley. Putting super-resolution fluorescence microscopy to work. *Nature Methods*, 6(1):21–23, 2009.

[7] J. Szymanski and M. Weiss. Elucidating the origin of anomalous diffusion in crowded fluids. *Phys. Rev. Lett.*, 103:038102, 2009.

[8] I. Golding and E.C. Cox. Physical nature of bacterial cytoplasm. *Phys. Rev. Lett.*, 96(9):098102, 2006.

[9] A.B. Fulton. How crowded is the cytoplasm? *Cell*, 30:345–347, 1982.

[10] I.M. Tolic-Nørrelykke, E-L. Munteanu, G. Thon, L. Oddershede, and K. Berg-Sørensen. Anomalous diffusion in living yeast cells. *Phys. Rev. Lett.*, 93(7):078102, 2004.

[11] H. van Beijeren and R. Kutner. Mean square displacement of a tracer particle in a hard-core lattice gas. *Phys. Rev. Lett.*, 55(2):238–241, 1985.

[12] Y. Suzuki, K. Kitahara, Y. Fujitani, and S. Kinouchi. Vacancy-assisted diffusion in a honeycomb lattice and in a diamond lattice. *J. of the Phys. Soc. of Japan*, 71(12):2936–2943, 2002.

[13] K. Seki and M. Tachiya. Reaction under vacancy-assisted diffusion at high quencher concentration. *Phys. Rev. E*, 80:041120, 2009.

[14] T. Ambjörnsson, L. Lizana, M.A. Lomholt, and R.J. Silbey. Single-file dynamics with different diffusion constants. *J. Chem. Phys.*, 129:185106, 2008.

[15] R. Kutner, K. Binder, and K.W. Kehr. Diffusion in concentrated lattice gases. ii. particles with attractive nearest-neighbor interaction on three-dimensional lattices. *Phys. Rev. B*, 26(6):2967–2980, 1982.

[16] K.W. Kehr, R. Kutner, and K. Binder. Diffusion in concentrated lattice gases. Self-diffusion of noninteracting particles in three-dimensional lattices. *Phys. Rev. B*, 23(10):4931–4945, 1981.

[17] R. Kutner and K.W. Kehr. Diffusion in concentrated lattice gases iv. diffusion coefficient of tracer particle with different jump rate. *Philosophical Magazine A*, 48(2):199–213, 1983.

[18] B. Jönsson, H. Wennerström, P.G. Nilsson, and P. Linse. Self-diffusion of small molecules in colloidal systems. *Colloid & Polymer Sci.*, 264:77–88, 1986.

[19] H. Berry. Monte Carlo simulations of enzyme reactions in two dimensions: Fractal kinetics and spatial segregation. *Biophys. J.*, 83:1891–1901, 2002.

[20] R. Phillips. *Physical Biology of the Cell*. Garland Science, 2009.

[21] N.J. Giordano and H. Nakanishi. *Computational Physics*. Pearson, 2006.

[22] J. Kurkijärvi and T.C. Padmore. Percolation in two-dimensional lattices. *J. Phys. A: Math. Gen.*, 8(5):683–696, 1975.

[23] B. Hughes. *Random Walks and Random Environments*, volume 2. Oxford University Press, 1995.

[24] A.C. Bebbington. A simple method of drawing a sample without replacement. *Appl. Statist.*, 24(1):136, 1975.

A Ergodicity

In order to find the analytic expression for the MSD in an ergodic system, we follow the discussion in section 3.1, and note that equation 2 may be written as:

$$\frac{1}{L_x L_y L_z}\left(\sum_{i=1}^{L_x} L_y L_z (x_i - x_0)^2 + \sum_{j=1}^{L_y} L_x L_z (y_j - y_0)^2 + \sum_{k=1}^{L_z} + L_x L_y (z_k - z_0)^2\right)$$

where each sum can be written as

$$\frac{1}{L_x}\left(\sum_{i=1}^{L_x} x_i^2 - 2x_0 \sum_{i=1}^{L_x} x_i + L_x x_0^2\right). \tag{8}$$

To solve the sum over the squared x-coordinate, $\sum x_n^2$, we use the Euler-Maclaurin summation formula:

$$\sum_{i=0}^{n} f(i) = \int_0^n f(x)dx - B_1\big(f(n) + f(0)\big) + \sum_{k=1}^{p} \frac{B_{2k}}{(2k)!}\Big(f^{(2k-1)}(n) - f^{(2k-1)}(0)\Big),$$

with $f(x) = x^2$. The B_k-coefficients are the Bernoulli numbers, and the last sum will be zero for all $p \geq 2$. From the summation formula we get $\sum x^2 = (n+1)(2n+1)n/6$. The remaining part of equation 8 is an arithmetic sum, which combined with previous result yields the final expression (for 1D):

$$\left\langle \delta x^2 \right\rangle = \frac{1}{6}(L_x + 1)(2L_x + 1) - 2x_0 \frac{(L_x + 1)}{2} + x_0^2,$$

where $\delta x = x_0 - x$. We get another term of the same form for each additional dimension, but with L_x interchanged for L_y, L_z, and x_0 for y_0, z_0.

B Algorithms Used

B.1 Without Interaction Between Particles

This is the algorithm used, in pseudocode, to model a many-particle system. Step 3 to 5 is a description of the *trial-and-error*-method, outlined in ref. [14].

1. We start by assigning jump rates to all particles, drawn from a distribution $\varrho(k)$, and construct a partial sum of all jump rates, such that:

$$\begin{aligned} p_0 &= 0 \\ p_n &= \sum_{i=1}^{n} k_i, \quad n = 1, \ldots 2dN \end{aligned} \tag{9}$$

   where k_i is the jump rate of the i:th particle and d the dimension.

2. Place the tagged particle at the center of the lattice, and position the remaining particles on the lattice, by using the Bebbington algorithm:

   > Cycle through all lattice sites (except the coordinates of the tagged particle), and place a particle at the current site with the probability n/m, where n is the number of particles left to place, and m is the number of lattice sites left to cycle through [24].

Set the time equal to zero.

3. Draw a random number $0 < r < 1$, with uniform distribution, and choose the jump rate k (which is uniquely defined for each particle and direction) such that
$$p_k \leq r p_{2dN} < p_{k+1}. \tag{10}$$
Next we want to determine the correct k by "trapping" $k_{\mathrm{g(uess)}}$ by moving our maximum and minimum values from right and left towards the correct k that will fulfill relation (10). Assign a left and right boundary, $p_L = p_0$ and $p_R = p_{2dN}$, and $k_L = 0$ and $k_R = 2dN$.

4. Draw a random number, $0 < r < 1$, with uniform distribution, and calculate a k_g to guess the value.
$$k_g = \frac{(r p_{2dN} - p_L)(k_R - k_L)}{p_R - p_L} + k_L.$$
If the condition of equation 10 is not fulfilled, we continue to either 4a or 4b:

   (a) If $r p_{2dN} < p_{k_g}$, move the right boundary,
   $$k_R = k_g$$
   $$p_R = p_{k_g}.$$

   (b) If $r p_{2dN} \geq p_{k_g+1}$, move the left boundary,
   $$k_L = k_g + 1$$
   $$p_L = p_{k_g+1}.$$

5. Repeat step 4 until relation (10) is fulfilled.

6. Convert k to corresponding particle and direction, and move it, according to the boundary conditions, and update the time to $t \to t + \frac{1}{p_{2dN}}$.

7. Move the particle back to its previous position if the new site is occupied.

8. Return to step 3 until $t = t_{\max}$.

9. Return to step 2 for the next ensemble, (for a quenched system).

B.2 With Interactions Between Particles

The following is an outline of a physically more correct interaction code, than what was used in section 7. This algorithm can form clusters that are mobile even when the binding energy tends towards infinity, and the cluster can break up into smaller parts, with a probability proportional to the number of bindings between the two (not yet formed) smaller clusters. To do this rigorously we should store all bindings between all particles and update these for each time step, which would result in a computationally slow algorithm. Instead we only assign bindings in the vicinity of the moving particle, thereby increasing the computational speed substantially.

1. Choose particle n to be moved, according to the jump rate distribution (see section B.1). If it does not have any nearest-neighbors we follow the method of the previous code.

2. If it does have a neighbor, we construct a cluster where each nearest-neighbor is included if the uniform random number $0 < r < 1$ fulfills (generate a new r for each neighbor):

$$r \geq \exp(-\beta \Delta \Phi).$$

3. For each particle added to the cluster we must check its neighbors, and repeat step 2 for them, until the bindings of each added particle has been checked. We make sure not to include any of the previously checked neighbor-bonds, otherwise detailed balance is broken, since looping over a previously checked, but excluded bond doubles its probability of being included in the cluster.

4. Form a sum of the friction coefficients (inverse jump rates) of the cluster particles and draw a new uniform random number r. Move the entire cluster if

$$r \leq \frac{k_n^{-1}}{k_n^{-1} + \sum_i k_i^{-1}}, \tag{11}$$

where k_n is the jump rate of particle n, originally chosen to be moved, and k_i represents the jump rate of the remaining cluster particles. If no move is made, continue to step 7.

5. If the condition in (11) was fulfilled we temporarily store the position of all cluster particles, and do a "trial-and-error" move with the entire cluster in the chosen direction. If there are no double occupancies we accept the move, and proceed to step 7.

6. If the new positions of the cluster particles are doubly occupied, we need to check whether the blocking particles should push the cluster back, or if the cluster pushes them forward. This is done by first checking the span of our cluster, perpendicular to the direction of movement, and include effects of the cluster being wrapped around the periodic boundary. All nearest-neighbors of the particles that are blocking the new position of the cluster should be included in a new "blocking cluster", provided they are within the left and right borders of the moving cluster, and not part of it, see figure 14. As in relation (11), we draw a uniform random number r, and move the cluster and all the blocking particles if:

$$r \leq \frac{\sum_i k_i^{-1}}{\sum_i k_i^{-1} + \sum_j k_j^{-1}},$$

where the summation index j runs over the jump rates of the blocking particles, and i runs over the moving cluster particles (now including particle n). If the condition is not fulfilled we move everything back to its original position.

7. Update the time as in the previous code B.1 (regardless of the success of the trial-and-error move), and return to step 1.

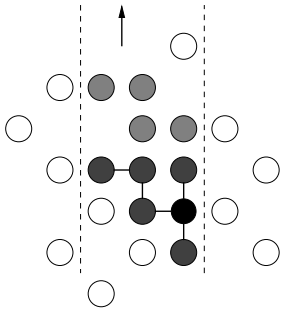

Figure 14: A model of our improved interaction algorithm. The black particle is the one chosen to be moved (particle n), and the dark grey particles represent the cluster that particle n is a part of. If the cluster is moved, in spite of it being blocked, it will push the blocking particles (light grey) in the movement direction.

C Choosing Simulation Values

The simulations in section 6 are rather heavy, so special heed must be taken to the aforementioned (section 3.1) restrictions on the time interval chosen, and how this relates to the lattice size. The interval $\tau_{\text{coll}} \ll t \ll t_{\text{eq}}$ can be somewhat loosely interpreted, therefore we perform simulations with constant concentration but on a larger lattice, for comparison. It will show us where our smaller system breaks down, which is where the result from the two simulations diverge.

We choose our simulation stopping time $t_{\max}$ differently depending on how fast the tracer particle moves, which in turn depends on how the friction coefficient of the surrounding media was chosen. For the uniformly distributed jump rates (sec. 6.1) we see from figure 15(a) that choosing $t_{\max} = 50$ for $k \leq 4$ gives the same result for both the small and the large lattice, and for $k > 4$, $t_{\max} < 30$ is adequate. For the power-law simulation (sec. 6.2) we can choose a higher $t_{\max}$ since the tracer particle is blocked by the heavy tailed distribution that generates particles with large friction constants. For $k \leq 2$ we chose $t_{\max} = 100$. For the interval $2 < k \leq 4$ we choose $t_{\max} = 50$, and for $4 < k \leq 6$, $t_{\max} = 30$.

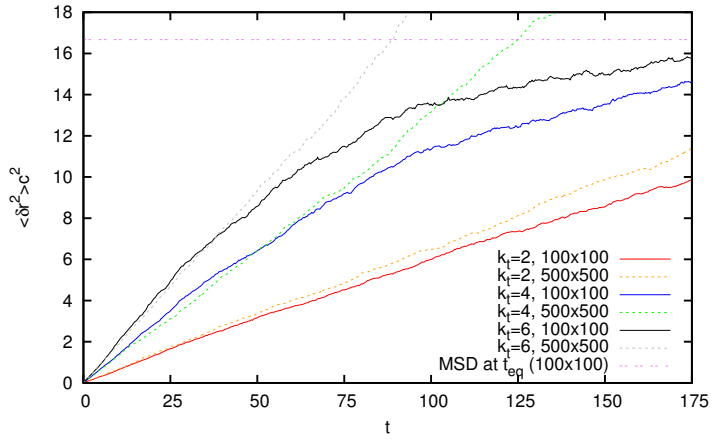

(a) uniform

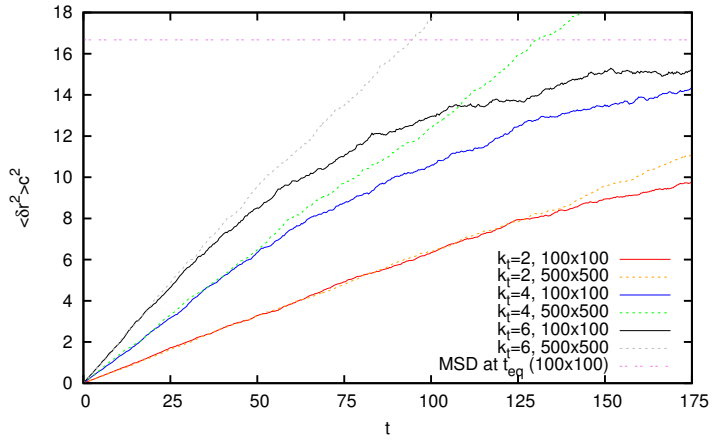

(b) power-law

Figure 15: Mean square displacement of a tracer particle, with $c = 0.1$, on a two dimensional lattice with 100×100 sites, compared against a 500×500-lattice, for three different jump rates, $k_t = 2$, $k_t = 4$, and $k_t = 6$; and for two different crowding distributions, uniform (fig. 15(a)), and a power-law (fig. 15(b)). At $t < 30$ both system sizes gives the same result for all jump rates, but at larger times the MSD for the smaller system deviates from the larger one, which is especially evident for the faster particle. The power-law was chosen with $\alpha = 0.5$, and the uniform was confined to the interval $0 < k_c < 1$. The horizontal line shows the MSD for the smaller system as it becomes ergodic. The MSD was averaged over 1000 ensembles.

D Supplementary Figures I

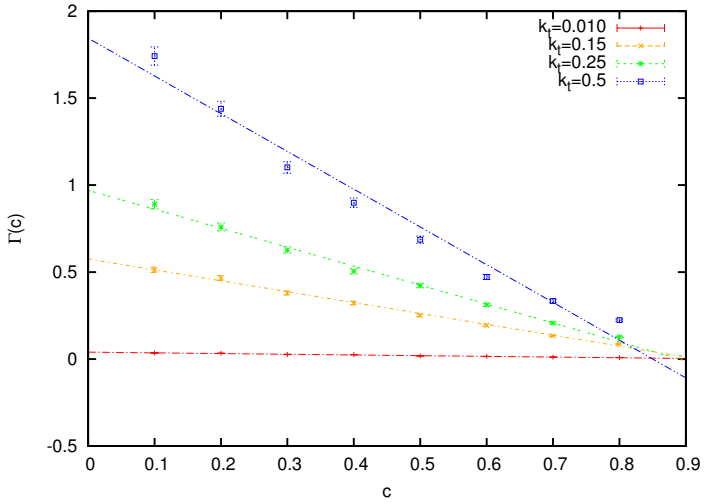

Figure 16: The concentration dependence of the diffusion constant seen in figure 9, where $\langle \delta r \rangle^2 = \Gamma(c)t$, together with three additional jump rates. The concentration dependence of the diffusion constant can roughly be fitted to a linear function.

E Supplementary Figures II

This section contains the individual MSD-plots of all simulations used in this thesis.

E.1 Nakazato Error Investigation

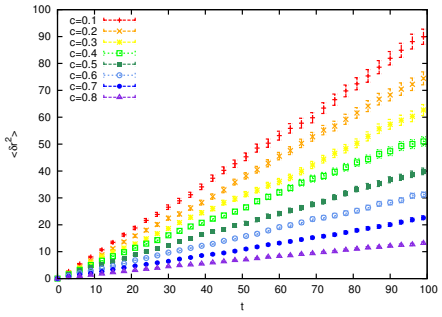

(a) $k = 0.5$

Figure 17: (Continued on the next page).

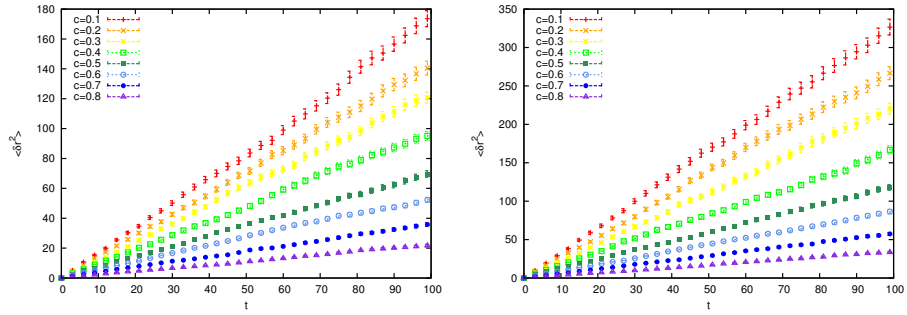

(b) $k = 1$

(c) $k = 2$

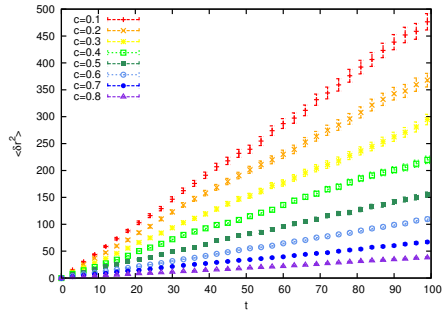

(d) $k = 3$

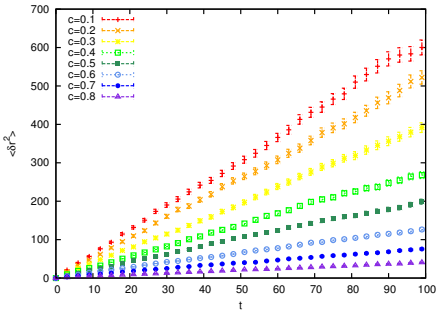

(e) $k = 4$

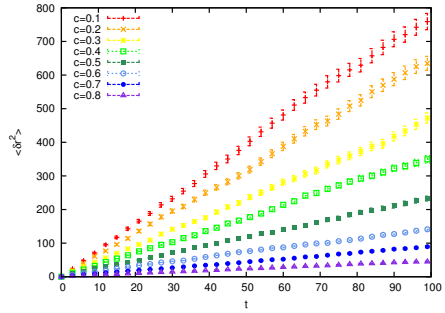

(f) $k = 5$

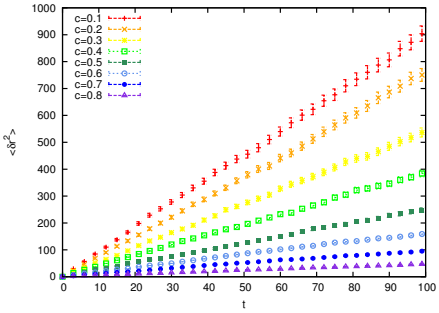

(g) $k = 6$

Figure 17: These are the individual simulation results which were reduced to figure 6, with jump ratio k, and concentration c varied. Simulations were performed on a 200×200-lattice, and the MSD was averaged over 1000 ensembles.

E.2 Simulations with Uniform Distribution

Figure 18: These are the individual simulation results from which we obtained figure 10. Figure 19(f) is the same as fig. 9 that could be seen in the main text.

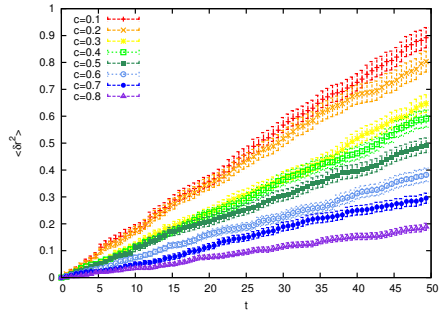

(a) $k_t = 0.005$

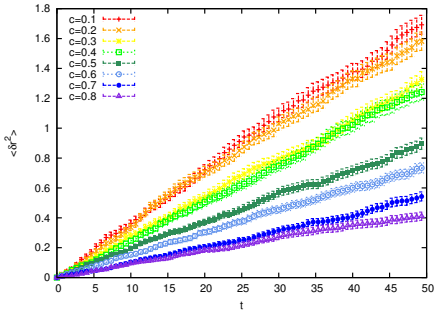

(b) $k_t = 0.01$

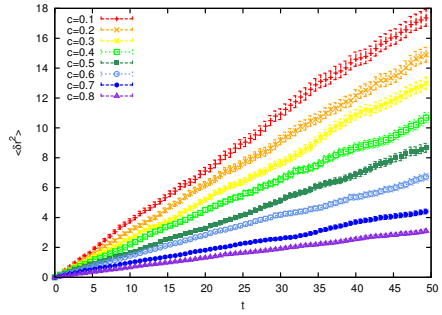

(c) $k_t = 0.1$

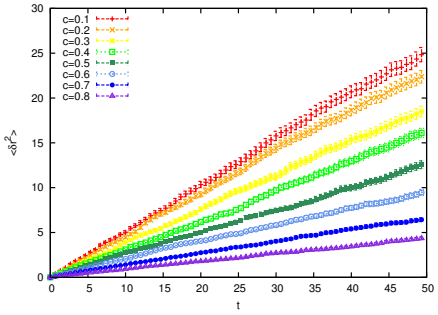

(d) $k_t = 0.15$

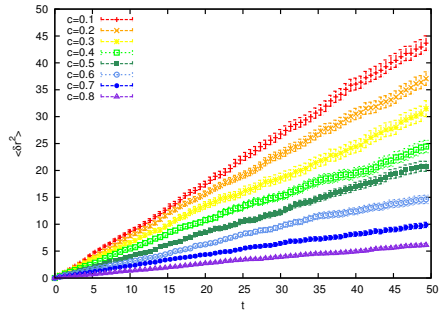

(e) $k_t = 0.25$

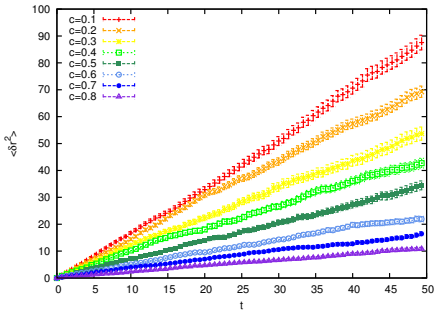

(f) $k_t = 0.5$

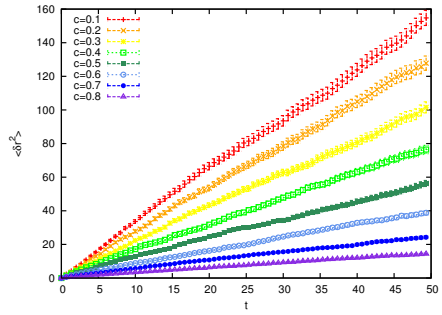

(g) $k_t = 1$

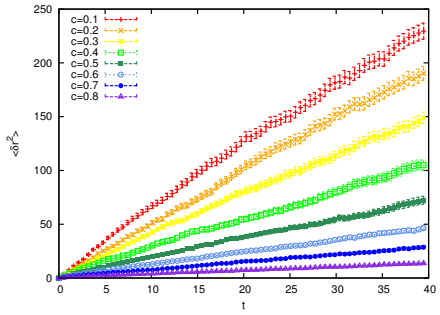

(h) $k_t = 2$

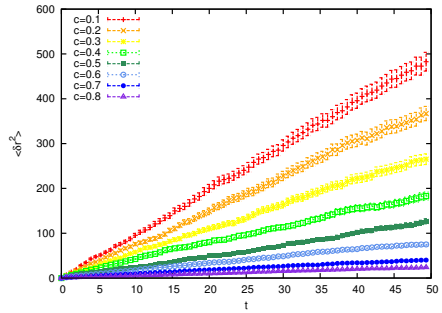

(i) $k_t = 3$

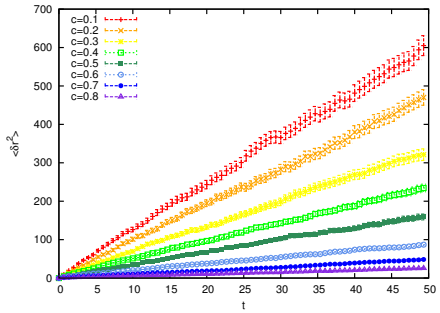

(j) $k_t = 4$

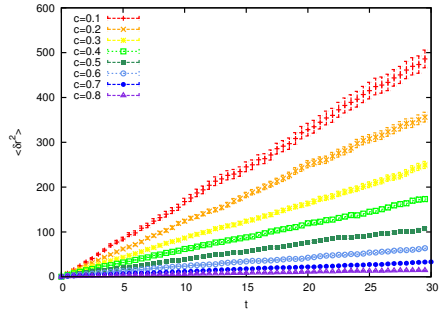

(k) $k_t = 5$

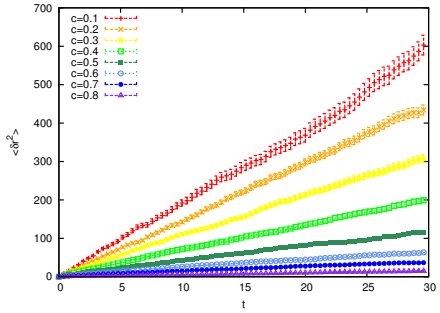

(l) $k_t = 6$

Figure 18: (Continued).

E.3 Simulations with Power-Law Distribution

Figure 19: These are the individual simulation results from which we obtained figure 11.

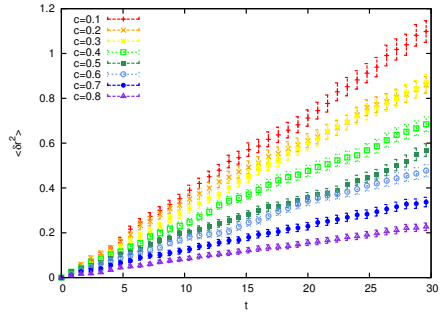

(a) $k_t = 0.01$

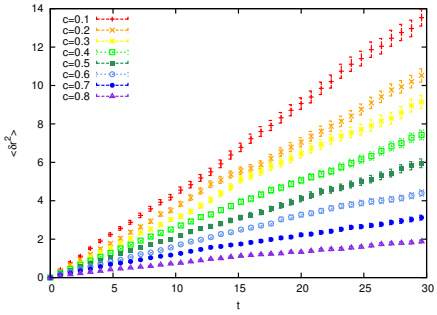

(b) $k_t = 0.10$

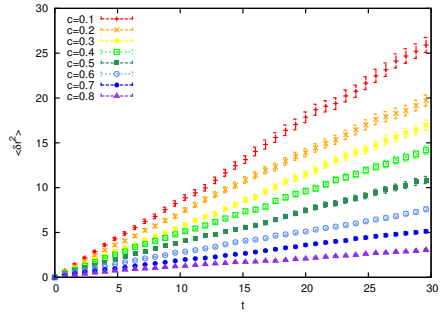

(c) $k_t = 0.25$

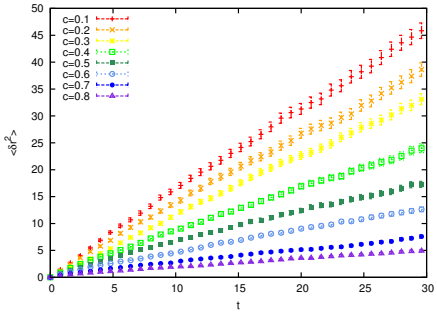

(d) $k_t = 0.5$

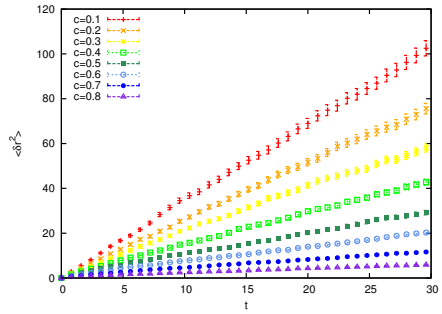

(e) $k_t = 1$

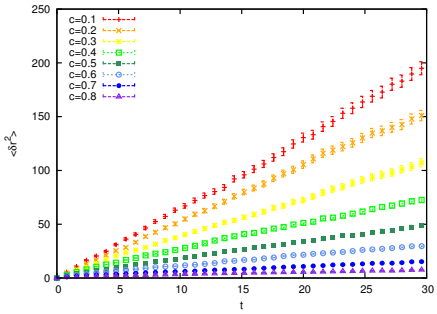

(f) $k_t = 2$

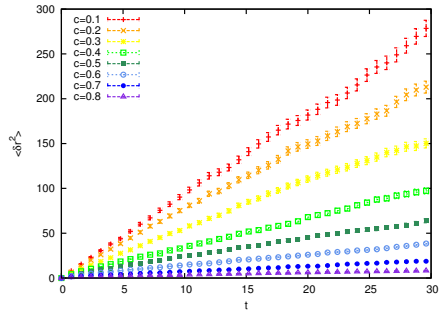

(g) $k_t = 3$

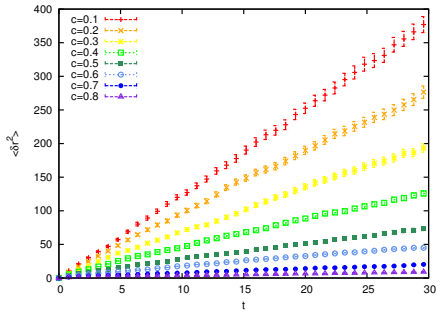

(h) $k_t = 4$

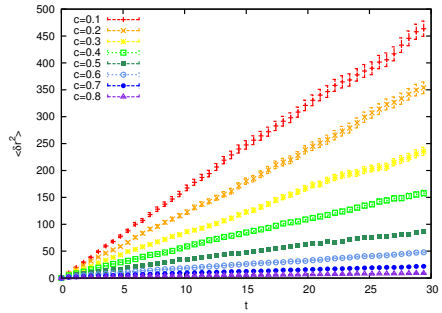

(i) $k_t = 5$

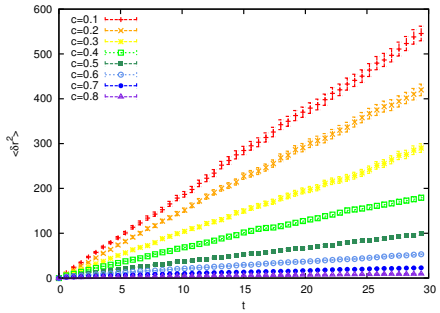

(j) $k_t = 6$

Figure 19: (Continued).

E.4 Interaction-plots

Figure 20: The result from each simulation, with different interaction strength, used to obtain figure 13.

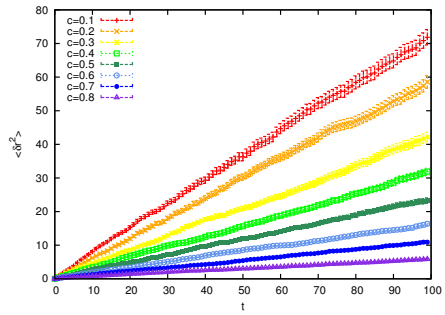

(a) $\beta\Delta\Phi = 0.25$

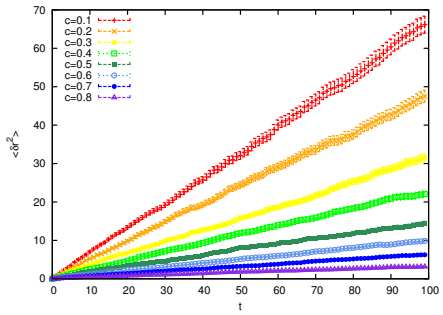

(b) $\beta\Delta\Phi = 0.5$

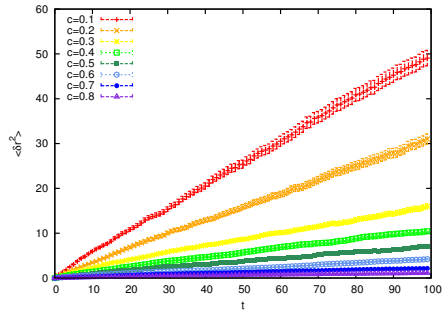

(c) $\beta\Delta\Phi = 1$

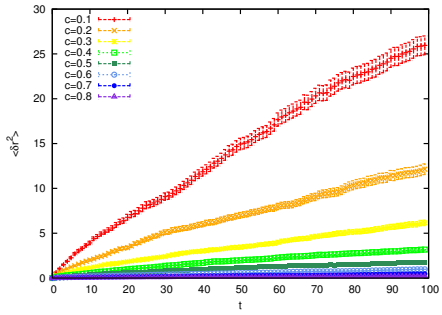

(d) $\beta\Delta\Phi = 2$

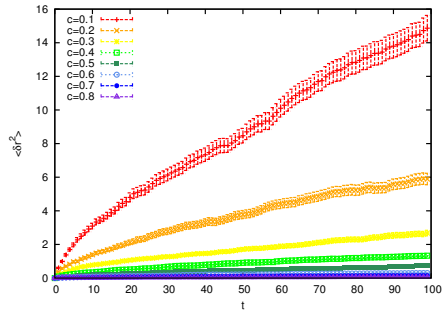

(e) $\beta\Delta\Phi = 3$

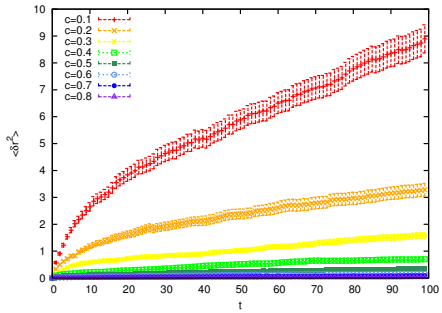

(f) $\beta\Delta\Phi = 4$

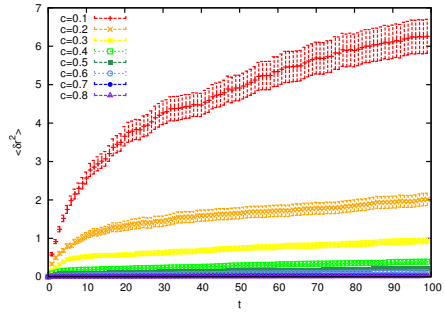

(g) $\beta\Delta\Phi = 5$

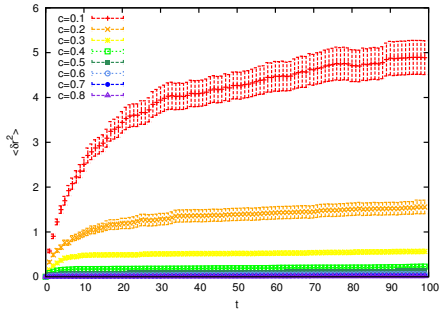

(h) $\beta\Delta\Phi = 6$

Figure 20: (Continued).